Topology GeometRics for the generation of the RoccustyrnaTM molecule, a ligand targeted COVID-19-D614G sites.

Ioannis Grigoriadis (Jgrigoriadis@biogenea.gr)
Biogenea Pharmaceuticals Ltd

Biological Sciences - Article

Keywords: COVID19, D614G, Gravitational, Topological, AI-Quantum computing, entanglement complexity computability, Quantum-Inspired Evolutionary Algorithm Predictive toxicology, QSAR, artificial intelligence, data mining, machine learning, datadriven, learning, chemoinformatics

Posted Date: December 1st, 2020

DOI: https://doi.org/10.21203/rs.3.rs-104212/v1

Topology GeometRics for the generation of the RoccustyrnaTM molecule, a ligand targeted COVID-19-D614G sites.1. Department of

BiogenetoligandorolQMMIDDD/QPRPICA/MACHNOT/

QIICDNNDCA ADMET/QIICDNNDCA Stations, Biogenea Pharmaceuticals Ltd - Greece.

Grigoriadis I.*

Keywords: COVID19, D614G, Gravitational, Topological, AI-Quantum computing, entanglement complexity computability, Quantum-Inspired Evolutionary Algorithm Predictive toxicology, QSAR, artificial intelligence, data mining, machine learning, datadriven, learning, chemoinformatics

Abstract

SARS coronavirus 2 (SARS-CoV-2) encoding a D614G mutation in the viral spike (S) protein predominate over time in locales where it is found, implying that this change enhances viral transmission. It has also been observed that retroviruses pseudotyped with SG614 infected ACE2-expressing cells markedly more efficiently than those with SD614. The availability of newer modeling techniques, powerful computational resources, and good-quality data have made it possible to generate reliable predictions for new chemical entities, impurities, chemicals, natural products, and a lot of other substances fuelling further development and growth of the field to balance the trade-off between the molecular complexity and the quality of such predictions that cannot be obtained by any other method. In this article, we effectively use a decision tree to obtain an optimum number of small chemical active chemical features from a collection of thousands of them utilizing a shallow neural network and jointly free energy cumulative feature ranking method with decision tree taking both network parameters and input toxicity benchmark features into account. In this paper, we strongly combine the toxic models and ADMET methods that are simple in machine learning characteristics, efficient in computing resource usage, and powerful to achieve very high accuracy levels for the in-silico generation of the RoccustyrnaTM small molecule, a less toxic nano-ligand targeted the COVID-19-D614G mutation using Topology Euclidean Geometric and Artificial Intelligence-Driven Predictive Neural Networks. To demonstrate this, we also develop a Gravitational Topological (UFs) based Quantum-Parallel Particle Swarm Inspired framework using only 2D chemical features that are less compute- intensive.

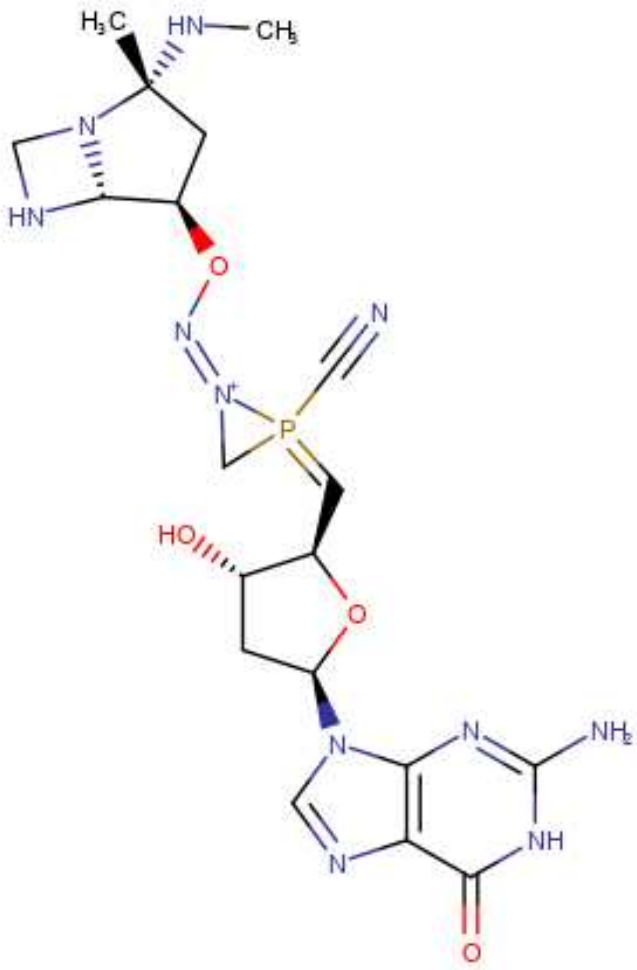

Introduction

The COVID-19 disease was declared on March 2020 a pandemic by the World Health Organization (WHO) and is accountable for a large number of fatal cases. (2,4) On January 2020, WHO emergency committee declared a global health emergency (3,4-6) based on the rate of increasing spread of the infection (4,5-7) with a reproductive number (RN) in the range 2.0-6.5, 4 higher than SARS and MERS, (8) with more than 85,000 casualties and fatality rate of about 4%.[1-4] Collaborative efforts for Genomic characterization, (5,6,7-9) Molecular epidemiology, evolution, phylogeny of SARS coronavirus and epidemiology from scientists worldwide are underway to understand the rapid spread of the novel coronavirus (CoVs), and to develop effective interventions for control and prevention of the disease. (1-10) Coronaviruses are positive-single stranded, enveloped large RNA viruses that infect humans and a wide range of animals. (7,8-11) Tyrell and Bonne reported the first coronavirus in 1966, (11) who cultivated the viruses from the patients suffering with common cold. (4,6,7-10) In Latin, Corona means “crown” based on their shapes. [1-12] Coronaviruses have four subfamilies, which includes alpha-, calculations.[2–13,14,15,16,17,18,19,20] Molecular structure can be determined in heterodox interpretations (22) by solving the time-independent (21-22) Schrödinger equation: QM methods, vertex prizes and edge costs including ab initio Density Filed Theories [DFT] (23) and semi-empirical in place (24) of the quantum processor and energy among other observables,(25) under simulated sampling error as well as to reposition drugs about bonding may represent the similarities (26) and dissimilarities(27) between drugs and repurposed viral proteins respectively. (28) However, the Schrödinger equation cannot actually be solved for any but a one- data-driven (29) electron system methods [the hydrogen atom], (30) and approximations need to be made. According to QM, [2-19,23] an electron bound that converges quickly and reliably to an atom cannot possess any [2-14,17,18,19-

29] arbitrary energy to produce the desired distribution by analyzing pharmacological data or occupy any position in space using statistical and machine [2-17,19,23,24-30] learning concepts. The Lindenbaum-Tarski algebra geometrically represented with logical spaces and has been previously introduced as a 3D logical space subspaces allowing a vectorial representation in which any one (of the eigenvalue statements) occupies a well-defined position and it is identified by a numerical ID. This shows the application to quantum computing through the example of three coupled harmonic oscillators allows pure mechanical computation both for generating rules and inferences. (25,26,27) It is shown that this abstract formalism can be geometrically represented with logical spaces and subspaces allowing a vectorial representation. (26,27,28-31) In general, the notions of Lindenbaum matrix and Lindenbaum-Tarski algebra have paved a way to further algebraization of logic, which had been begun by George Boole in the 19th century, as well as to a new branch of logic, model theory.. Philosophical interpretations of QM were conditioned by ideals of what an explanatory theory should be. (Minkowski-type, wave-edge, etc), (29,30,32-33) as well as probabilistic transformations Algebraic multi-metrics (Triangle area, Bond-angle, etc) and the associated axiomatic formulations (AQFT) treat observables rather than states as foundational for the interaction information extraction. (29,33,34,35) In this project, we show the application to quantum computing through the example of three coupled harmonic oscillators as orthogonical applied for the design of a novel multi-chemo-structure against the crystal structure of COVID-19 protein targets in a Lindenbaum-Tarski generated QSAR automating modeling lead compound design approach. (29,32,33,35,36) A generalized procedure of Quantization of classical fields that was fused together with QSAR automating modeling as proposed to lead the commutation and anticommutation relations and a C* algebra of local observables. (36,37,39,40,41,42) States were defined as linear functionals on the algebra of free energy docking observables. Docking Interactions were used in this project and filtered proteins on several parameters, for Supercritical entanglement introduced in this word to the area law for an advanced quantum mechanical inverse docking algorithm to confirm the practicality of the docking energy predictions.

Materials and Methods

Preparation of the protein structures

We provided to the DockThor-VS users the structures of some SARS-CoV-2 (1,3-10) potential therapeutic targets (2,3,5-11_ for the design of new drugs and vaccines. (1,3-9) For this purpose, we initially select the non-structural proteins Nsp3, Nsp5 (PLpro domain), Nsp12 (RdRp) and Nsp15 (endoribonuclease), (1-4,6,7-24) and the structural proteins Spike and nucleocapsid protein (N protein). (3,7,9-20)) For this purpose, we clustered the opened states (31 out of 40 states) (3-9,17,21) using the Conformer Cluster tool in BiogenetoligandorolTM (BiogenetoligandorolTM, SynthocureTM, Thessaloniki, Biogenea Pharmaceuticals Ltd-GR, 2020) (14,16-29,32) according to the position of the residues (3-11,23-37) Arg102 and Tyr109 using the weighted centroid as the linkage method. (4-12,29) Finally, the nearest to the centroid structure per cluster was selected as the representative conformation of each group to be available at BiogenetoligandorolTM. In this work, we prepared the protein structures using the Protein Preparation Wizard from the BiogenetoligandorolTM (BiogenetoligandorolTM, SynthocureTM, Thessaloniki, Biogenea Pharmaceuticals Ltd-GR, 2020). (4,6-17-39) Protonation assignment and hydrogen-bond optimization were performed using ProtAssign and PROPKA 84 at the reported experimental pH and (23-39,41) considering the presence of the bound ligand when available (5,7-8,12).

Screening NuBEE Phyto-library and COVID2019 targets.

Molecular docking and quantum mechanical Schrodinger-inspired physarum-prize-collecting Neural Matrix Factorization drug repositioning scoring analysis are implemented to a collection of the Natural Products of the Chemistry Institute of UNESP, Araraquara/SP. Virtual screening is a technique largely based on its libraries of small molecules and the COVID19 target sites. (2,4,5-10) Protein-molecule complexes, (4,5,7,8-13) followed by structural relaxation were generated through (8,10,13-14) flexible-ligand:rigid-receptor molecular docking (9,13,15,16-19) in this local energy minimization to optimize

protein-ligand interactions capping the N- and C-terminal of each active fragment with i-GEMDOCK (13,18,19-24,26) through cycles in amino-acids within 4 Å of any docked molecule as considered free of local energy minimization. (2,5-21) By using the ChEMBL database, 10 best keyword matching the compounds (Table1) were obtained namely, Colchicine, Raltegravir,, Hexacosanol, Benzoxazolinon, Carboxy-Pentaric acid, Ursane, Antheraxanthin, RA-XIII, Crotonate and Byrsonima Coccolobifolia against the SARS-COV-2 protein targets of the (pdb:1xak), (pdb:6xs6) and (pdb:6lu7). (6,7-27) For each target, all amino-acids of the cut-out system with hydrogens were then collected, within 8 Å of any docked molecule and used to build a reduced system where the “o” subscript in the first term refers to the difference of the free energy calculated using the protein-ligand (PL), protein (P) and ligand (L) conformations and GQM (X) is the energy of X from the docked complex, in the free unbound state the fourth term corresponds to the change in conformational entropy, were generated and the second and third unbound states are calculated through local energy minimization as ΔGQMconf (X) = GQMo(X)− GQM (X) ,(X = L, P) (2) where GQMo (X) is the energy of the isolated X in the conformation of the docked PL on both protein and molecule complex Inhibitors from the Bioactivity-Guided Fractionation of the Colchicine, Raltegravir, Hexacosanol, Benzoxazolinon, Carboxy-Pentaric acid, Ursane, Antheraxanthin, RA-XIII, Crotonate and Byrsonima coccolobifolia Leaves and Stems to be fragmented, recored and accordingly merged into the RoccustyrnaTM small hyperactive druggable scaffold. The acknowledgement of the binding of the selected 8 phytical compounds to their target proteins was accomplished using Molinspiration (http://www.molinspiration.com/cgi-bin/properties) and DrugBank (10,11).

Pharmacophoric-ODEs fragmentating, merging and recoring : Biogenetoligandorol AI-heuristic algorithm.

The patterns of this Biogenetoligandorol fragmentation scheme are sorted into the workings of the Galilean transformation by examining the “extended” Galilean transformation based on a set of heuristically determined descriptors to a rigid system having an arbitrary time-dependent acceleration. These descriptors can be, for example, the number of atoms describing the pattern and be determined by the substitution ip(r, t) = eiJ{r,t) (p(r', t). V'ip = (V'ip + iV 'f) eif, V'2ip = {V'2ip + 2iV'f-V'(p+(pV'2f+ <p(V'f)2)e‘f,i>= (f)+ if<p) eif,and the Schrödinger equation becomes n 2 2 m (V,z(p + 2 iV'f-V'(p+ i(pV f - (V 'fY <p)= ifi [(<p + if(p) -g.(V '(p + i(pv' f)] where p+2 are the the number of bonds available or the number of double bonds. The complete fragmentation scheme is analyzed to find patterns that are contained within the selected 10 hit compounds of the Colchicine, Raltegravir, Hexacosanol, Benzoxazolinon, Carboxy-Pentaric acid, Ursane, Antheraxanthin, RA-XIII, Crotonate and Byrsonima coccolobifolia. Whenever searching for a specific pattern, if the group has such a parent pattern, the parent pattern is searched first eliminate the terms in V'(p,which gives f = — %-r'+ g(t). Then one can choose n g{t) such as to eliminate the purely time-dependent terms, and one finally arrives at, = * (2mV '2(p + mf; ■ r'(p = ih(p,ipir, t) =— ea h J (pir',t). (34-42) of the strong equivalence principle in quantum theory. After that, the child pharmacophoric pattern is searched in an inertial repeated merged system S asip = % (ml5 r, t) + ip2im2, r, t). (21-42)Then assume that one fragmented pharrmacophore can describe the same superposition in an accelerating to a larger ligand-receptor system S' that obeys (14), with § = £(r), £(0) = £(7) = 0, so that the system S' performs a closed quantum circuit and coincides with the chemical structure system the S at times t = 0 and t=T, such that r ’ iT) = r(7). (25-34,37) To avoid incomplete group assignments, whenever a part of the structure is already fragmented, the subsequent matches have to be adjacent to the groups already found. (26,31-39) As a first step, the algorithm performs a quick search for the different groups in the fragmentation scheme applying the heuristic group prioritization and the parent–child group prioritization as described above. (29,32-39) The search goes sequentially through the sorted fragmentation scheme, adding groups that are found and do not overlap with groups that were already found. In case it successfully finds a valid fragmentation, this is taken as the solution merely relating to how one would describe the same state in a different coordinate system. (33,35-42) This Lindenbaum-Tarski algebraic algorithm was implemented as a recursive algorithm that performs a complete tree search of all possible combinations of fragmentation, merging and pharmacophoric recoring systems. To reduce the

fragmentation space that needs to be searched, the algorithm of the two independent Chern-Simons actions with group on the heuristic level of path integrals, was applied where the partition function is the modulus square of the partition function for the Chern-Simons theory whichWitten famously associated with knot theory keeps track of the solutions already found and of the selected group of drug combinations which be superposed in non-relativistic quantum mechanics that lead to the complete fragmentation. (21,33,36,38-42) If several chemical solutions were found in the end, the theory has a sequence of similar such spaces of finite but arbitrarily large dimension, where the dimension increases with the resolution of relative measurements to the first system of the 10 hit selected small molecules the possible chemical solutions were sorted by the number of different patterns and the first solution was taken as the determined fragmentation. (36,37,39-41,42) This way, patterns with larger groups are prioritized over smaller chemical pattenrs with potential antiviral properties of the: (1Z)-2-{[(2S,3S,5R)-5-(2-amino-6-oxo-6,9-dihydro-3H-purin-9-yl)-3-hydroxyoxolan-2-yl]methylidene}-2-cyano-1-({[(2S,4R,5R)-2-methyl-2-(methylamino)-1,6-diazabicyclo[3.2.0]heptan-4-yl]oxy}imino)-1lambda5,2lambda5-azaphosphiridin-1-ylium patterns.

Results

In this study we have shown that the QMMM designed Roccustyrna small molecule which was designed in silico by using Topology Euclidean Geometric and Artificial Intelligence-Driven Predictive Neural Networks was engaged in the binding domains of the protein targets of the (pdb:1xak) with the docking energy values of the (T.Energy, I.Energy, vdW, Coul, NumRotors, RMSD, Score), (-19.625, -35.483, 7.633, -43.116, 7, -5.813)Kcal/mol, (Tables1a,1b,2a) The Roccustyrna chemical structure interacted into the binding sites of the protein targets (pdb:6W9C) with the negative docking energies of the (T.Energy, I.Energy, vdW, Coul, NumRotors, RMSD, Score), (-36.678 ,-55.648, -7.519, -48.129, 7, -6.762) Kcal/Mol. It also generated **Hydrophobic Interactions** | when docked onto the binding cavities of the amino acid of the 168 | PRO | A | 1 | 02J | C | with the docking energy values of the 3.53 | 2369 | 1303 | -10.425, 3.420, 72.447 | -13.394, 3.190, 70.551 |. Our new QMMM designed small molecule named Roccustyrna involved in the generation of the hydrogen bonding within the PJE:C:5 (PJE-010) + 010:C:6 Interacting chain(s) while generating **Hydrophobic Interactions** when docked into the binding domains of the amino acid of the | 25 | THR | A | 6 | 010 | C | with the docking energy values of the 3.73 | 2415 | 179 | -7.156, 21.406, 66.898 | -8.709, 22.779, 70.002 |Kcal/mol. The Roccustyrna's active pharmacophoric site of the (methylamino)-1,6-diazabicyclo[3.2.0]heptan-4-yl]oxy}imino) interacted into the binding cavities of the amino acid of the | 26 | THR | A | 6 | 010 | C | with the docking energy values of the 3.81 | 2415 | 186 | -7.156, 21.406, 66.898 | -6.155, 24.392, 64.757 |Kcal/mol. The Roccustyrna's active pharmacophoric site of the dihydro-3H-purin-9-yl)-3-hydroxyoxolan generated an inhibitory effect which was involved in the generation of **Hydrogen Bonds**| when docked into the binding cavities of the amino acid of the 143 | GLY | A | 6 | 010 | C with the docking energy values of the 1.93 | 2.80 | 145.29 1105 | Nam | 2411 | O3 | -8.911, 17.849, 65.703 | -8.918, 17.918, 62.905 | | 164 | HIS | A | 5 | PJE | C 2.16 | 3.07 | 153.73 2408 | N3 | 1266 | O2 | -12.282, 14.994, 67.123 | -15.161, 15.336, 68.144 |. 6LU7 02J:C:1 (02J) Interacting chain(s): A and **Hydrophobic Interactions** within the binding domains of the amino acid of the | 168 | PRO | A | 1 | 02J | C | with the docking energy values of the 3.53 | 2369 | 1303 | -10.425, 3.420, 72.447 | -13.394, 3.190, 70.551 | PJE:C:5 (PJE-010) + 010:C:6 Interacting chain(s): A C The Roccustyrna's pharmacophoric active site of the 2-lambda5-azaphosphiridin-1-ylium was engaged in hydrogen bonding interactions with the **Hydrogen Bonds**| 143 | GLY | A | 6 | 010 | C 1.93 | 2.80 | 145.29 1105 | Nam | with the docking energy values of the | 3.81 | 2415 | 186 | -7.156, 21.406, 66.898 | -6.155, 24.392, 64.757 | 2411 | O3 | -8.911, 17.849, 65.703 | -8.918, 17.918, 62.905 | | 164 | HIS | A | 5 | PJE | C 2.16 | 3.07 | 153.73 2408 | N3 | 1266 | O2 | -12.282, 14.994, 67.123 | -15.161, 15.336, 68.144 |Kcal/mol. The Roccustyrna small molecule involved in the generation of the **Hydrophobic Interactions** within the binding domains of the amino acid of the | 25 | THR | A | 6 | 010 | C | with the docking energy values of the 3.73 | 2415 | 179 | -7.156, 21.406, 66.898 | -8.709, 22.779, 70.002Kcal/mol as illustrated in the figures of this in silico drug design project (Figures1,2a,2b,2c,2d,3a,3b,3c,4a,4b,5a,5b,5c,5d,6a,6b,6c,6d,6e). In this project, we generated the

Quantum Heuristic Fragmentation Algorithms for the merging and recoring of the hit selected FDAs and Drug Pair Interactions by using Quantum Hamiltonians of the =γB·(Sˆ1+Sˆ2)+Iˆ·A·Sˆ2, Sˆi=(σx,σy,σz)Iˆρs(t)=TrI[U(t)ρ(0)U†(t)],ρI(0)=I/2P(t′)=dΔM(t′)ΔM=f(t′)dt′,ρ¯s=∫−∞0f(t′)ρs(t′)dt′=∫0∞ f(t)ρs(t)dt,∫−∞0f(t′)dt′=∫0∞f(t)dt=1ρ¯sρ¯sρ¯sρ¯s[0,π/2]ρ¯sρs(0)ρ¯sQFI≈∑i=01Re[ρi12]2(1ρi11+1ρi22) +(ρi11−ρi22)2ρi11+ρi22,ρ1ij= 〈φi| 〈1|ρs(0)|φj〉 |1〉 ρ0ij= 〈φi| 〈0|ρs(0)|φj〉 |0〉 |0〉 |1〉 H1=γB0·S ˆ1Re[ρi12]ρi12ρs(0)ρ¯s|S〉 =12(|10〉 −|01〉)30%ρs(0)ρ¯s=H⊗m|0〉 ⊗m=H⊗H⊗⋯⊗H|00⋯0〉 = 12(|0〉 +|1〉)⊗12(|0〉 +|1〉)⊗⋯⊗12(|0〉 +|1〉)=12m(|00⋯0〉 +|00⋯1〉)+⋯+(|11⋯1〉) In this article we generated the RoccustyrnaTM small molecule (Fig1-Fig8) with the Geometrical Descriptors of the: Dreiding energy = 305,20 kcal/mol, MMFF94 energy = 35,06 kcal/mol, Minimal projection area = 66,49, Maximal projection area = 123,65 Minimal projection radius = 5,71 Maximal projection radius = 9,24 Length perpendicular to the max area = 10,29 Length perpendicular to the min area = 19,04 van der Waals volume = 409,41 Donor count = 5 Donor sites = 6 Acceptor count = 11 Acceptor sites = 14. Finally, the Roccustyrna chemical structure generated an inhibitory docking effect of high negative binding energy docking values of the -66,7 Kcal/mol when docked onto the cav7bv2_POP binding domains within the amino acids of the V-M-LYS-551, V-S-LYS-551, V-S-ARG-553, V-S-ASP-618, V-M-TYR-619, V-M-PRO-620 with the docking energy values of the -4.71516, -10.4842, -4.7999, -6.65538, -5.1339, -6.28532Kcal/mol. On the other hand the Remdesivir drug when combined to the Roccustyrna small molecule interacted at the same binding domains of the amino acids of the V-M-LYS-551, V-S-LYS-551, V-S-ARG-553, V-S-ASP-618, V-M-TYR-619, V-M-PRO-620 with positive and zero docking values of the +42.1, -0.104885, -0.19986, +25.0575, 0, 0, 0Kcal/mol. That means that the Remdesivier drug in same cases could induce the COVID19 disease.

Discussions

In this article, we propose an alternative topological quantum computing optimization framework for the computation of topological invariants of knots, links and tangles through a stochastic discrete optimization procedure that uses ground structure approach, nonlinear finite element analysis, and quantum-inspired evolutionary algorithms in which the concepts of proper time and rest mass enter in the non-relativistic limit. The focus of this work is to develop a fragmentation algorithm that is as independent as possible from the chosen fragmentation scheme to allow for a faster development of new group contribution methods. For this reason, the Roccustyrna mutli-targeted pharmacophoric element for each pattern was kept as simple as possible and can be geometrically represented with logical atomic spaces and subatomic subspaces allowing a vectorial negative docking energy representation. The few chemical patterns (that were made more specific to match the results better from the literature database have been underlined in this project as orthogonically applied for the design of a novel multi-chemo-structure the Roccustyrna small molecule against the crystal structure of COVID-19 main protease in complex with an inhibitor N3 in a Lindenbaum-Tarski generated generated QSAR automating modeling lead compound design approach. In this hybrid drug designing approach, we have designed the RoccustyrnaTM nano-structures as a system of intrinsically positioned cables filtered before evaluation and triangular bars kinematically stable and structurally valid symmetric formations of connected components, holes, and voids jointed at their ends by hinged connections to form a rigid chemical scaffold for calculating Betti numbers—the numbers—in persistent homology.

Conclusions

Here, for the first time we have generated three coupled harmonic oscillators as orthogonically applied for the design of a quantum thinking novel multi-chemo-structure against the crystal structure of COVID-19 main protease, the RoccustyrnaTM small molecule by applying the Biogenetoligandorol algorithm, a Gravitational Topological (UFs) based Quantum-Parallel Particle Swarm Inspired framework using only 2D chemical features that are less compute- intensive in which a generalized procedure of Quantization of classical heuristic fields that can be fused together with QSAR automating modeling. (31-42) The strategies developed and implemented for the two algorithms using

Topology Euclidean Geometric and Artificial Intelligence-Driven Predictive Neural Networks in this work, show that it is possible to automate group fragmentation based on computed descriptors for the patterns in the fragmentation scheme to make use of partial chemical derivatives with the additional difficulty that the drug designs we deal with are not orthogonal. (30-42) Both algorithms applied in this project are capable of fragmenting every molecule of a reference database of structures into their respective UNIFAC groups. Furthermore, the heuristic algorithms which were used in this project are capable of fragmenting and remerging small molecules that could not be fragmented by the algorithm of the reference database. (2,5-42) We have illustrated the power of such an approach interpreted as distinct quantum circuit, qubit preparations, and certain 1- and 2-qudit gates in a meaningful application to components, such as qubits. Our Biogenetoligandorol platform also offers utility to researchers simply wishing to interrogate and organize generalized Hadamard and control-Z gates data, as it can be applied to create an inventory of available numerical docking data with particular clinical or genomic features, of the shaded tangle into two-dimensional space such as available datasets or patients with particular mutations, which may be used to draw independently of its drug identification capabilities. (26,29-42) More specifically, in this project we implemented Inverse Docking Algorithms with nonlinear electrodynamics indicated to us that the RoccustyrnaTM small molecules exert the highest inhibitory activities and negative docking energies as compared to other FDAs against the same SARS-COV-2 viruses protein targets and while it is probably true that the injudicious use of these ideas can cause problems, it is also true that they do and should play a role quantum mechanically in the this drug discovery field.

REFERENCES

1. Hui DS. Epidemic and Emerging Coronaviruses (Severe Acute Respiratory Syndrome and Middle East Respiratory Syndrome). Clin Chest Med. 2017;38(1):71-86.

2. Zhu N, Zhang D, Wang W, Li X, Yang B, Song J, Novel Coronavirus from Patients with Pneumonia in China, 2019. N Engl J Med. 2020;382(8):727-33.

3. Paraskevis D, Kostaki EG, Magiorkinis G, Panayiotakopoulos G, Sourvinos G, Tsiodras S. Full-genome evolutionary analysis of the novel coronavirus (2019-nCoV) rejects the hypothesis of emergence as a result of a recent recombination event. Infect Genet Evol. 2020;79:104212.

4. Lu R, Zhao X, Li J, Niu P, Yang B, Wu H, G enomic characterisation and epidemiology of 2019 novel coronavirus: implications for virus origins and receptor binding. Lancet. 2020;395(10224):565-74.

5. Luk HKH, Li X, Fung J, Lau SKP, Woo PCY. Molecular epidemiology, evolution and phylogeny of SARS coronavirus. Infect Genet Evol. 2019;71:21-30.

6. Ziebuhr J. Molecular biology of severe acute respiratory syndrome coronavirus. Curr Opin Microbiol. 2004;7(4):412-9.

7. Weiss SR, Leibowitz JL. Coronavirus pathogenesis. Adv Virus Res. 2011;81:85-164.

8. Brian DA, Baric RS. Coronavirus genome structure and replication. Curr Top Microbiol Immunol.2005;287:1-30.

9. Narayanan K, Huang C, Makino S. SARS coronavirus accessory proteins. Virus Res.2008;133(1):113-21.

10. Arndt AL, Larson BJ, Hogue BG. A conserved domain in the coronavirus membrane protein tail is important for virus assembly. J Virol. 2010;84(21):11418-28.

11. Neuman BW, Kiss G, Kunding AH, Bhella D, Baksh MF, Connelly S, et al. A structural analysis of M protein in coronavirus assembly and morphology. J Struct Biol. 2011;174(1):11-22.

12. Siu KL, Chan CP, Kok KH, Chiu-Yat Woo P, Jin DY. Suppression of innate antiviral response by severe acute respiratory syndrome coronavirus M protein is mediated through the first transmembrane domain. Cell Mol Immunol. 2014;11(2):141-9.

13. Schoeman D, Fielding BC. Coronavirus envelope protein: current knowledge. Virol J. 2019;16(1):69.

14. Al-Tawfiq JA, Al-Homoud AH, Memish ZA. Remdesivir as a possible therapeutic option for the COVID-19. Travel Med Infect Dis. 2020:101615.

15. Agostini ML, Andres EL, Sims AC, Graham RL, Sheahan TP, Lu X, et al. Coronavirus Susceptibility to the Antiviral Remdesivir (GS-5734) Is Mediated by the Viral Polymerase and the Proofreading Exoribonuclease. mBio. 2018;9(2).

16. de Wit E, Feldmann F, Cronin J, Jordan R, Okumura A, Thomas T, et al. Prophylactic and therapeutic remdesivir (GS-5734) treatment in the rhesus macaque model of MERS-CoV infection. Proc Natl Acad Sci U S A. 2020.

17. Kim JY. Letter to the Editor: Case of the Index Patient Who Caused Tertiary Transmission of Coronavirus Disease 2019 in Korea: the Application of Lopinavir/Ritonavir for the Treatment of COVID-19 Pneumonia Monitored by Quantitative RT-PCR. J Korean Med Sci. 2020;35(7):e88.

18. Khot WY, Nadkar MY. The 2019 Novel Coronavirus Outbreak - A Global Threat. J Assoc Physicians India. 2020;68(3):67-71.

19. Zeng YM, Xu XL, He XQ, Tang SQ, Li Y, Huang YQ, et al. Comparative effectiveness and safety of ribavirin plus interferon-alpha, lopinavir/ritonavir plus interferon-alpha and ribavirin plus lopinavir/ritonavir plus interferon-alphain in patients with mild to moderate novel coronavirus pneumonia. Chin Med J (Engl). 2020.

20. Wang Z, Chen X, Lu Y, Chen F, Zhang W. Clinical characteristics and therapeutic procedure for four cases with 2019 novel coronavirus pneumonia receiving combined Chinese and Western medicine treatment. Biosci Trends. 2020;14(1):64-8.

21. Martinez MA. Compounds with therapeutic potential against novel respiratory 2019 coronavirus. Antimicrob Agents Chemother. 2020.

22. Gordon CJ, Tchesnokov EP, Feng JY, Porter DP, Gotte M. The antiviral compound remdesivir potently inhibits RNA-dependent RNA polymerase from Middle East respiratory syndrome coronavirus. J Biol Chem. 2020.

23. Sheahan TP, Sims AC, Leist SR, Schafer A, Won J, Brown AJ, et al. Comparative therapeutic efficacy of remdesivir and combination lopinavir, ritonavir, and interferon beta against MERS-CoV. Nat Commun. 2020;11(1):222.

24. Trott O, Olson AJ. AutoDock Vina: improving the speed and accuracy of docking with a new scoring function, efficient optimization, and multithreading. J Comput Chem. 2010;31(2):455-61.

25. Van Meter R, Satoh T, Ladd TD, Munro WJ, Nemoto K (2013) Path selection for quantum repeater networks. Networking Science 3(1-4): 82-95.

26. Lloyd S, Mohseni M, Rebentrost P (2014) Quantum principal component analysis. Nature Physics. 10: 631.

27. Howlader P, Banerjee M. Object Oriented Protoconcepts and Logics for Double and Pure Double Boolean Algebras. Rough Sets. 2020;12179:308-323. Published 2020 Jun 10. doi:10.1007/978-3-030-52705-1_23

28. Gyongyosi L (2017) Quantum Imaging of High-Dimensional Hilbert Spaces with Radon Transform. International Journal of Circuit Theory and Applications 45(7): 1029-1046.

29. Yuan Z (2008) Experimental demonstration of a BDCZ quantum repeater node. Nature 454: 1098-1101.

30. Di Caro G, Ducatelle F, Gambardella LM (2005) AdHocNet: An Adaptive Nature-Inspired Algorithm for Routing in Mobile Ad-Hoc Networks. European Transactions on Telecommunications 16: 443-455.

31. Chou C (2007) Functional quantum nodes for entanglement distribution over scalable quantum networks. Science 316(5829): 1316-1320.

32. Kimble HJ (2008) The quantum Internet. Nature 453: 1023-1030.

33. Gyongyosi L (2014) The Correlation Conversion Property of Quantum Channels. Quantum Information Processing 13: 467-473.

34. Kok P (2007) Linear optical quantum computing with photonic qubits. Rev Mod Phys 79: 135-174.

35. Gisin N, Thew R (2007) Quantum Communication. Nature Photon 1: 165-171.

36. Enk SJ, Cirac JI, Zoller P (1998) Photonic channels for quantum communication. Science 279: 205-208.

37. Briegel HJ, Dur W, Cirac JI, Zoller P (1998) Quantum repeaters: the role of imperfect local operations in quantum communication. Phys Rev Lett 81:5932-5935.

38. Dur W, Briegel HJ, Cirac JI, Zoller P (1999) Quantum repeaters based on entanglement purification. Phys Rev A 59: 169-181.

39. Duan LM, Lukin MD, Cirac JI, Zoller P (2001) Long-distance quantum communication with atomic ensembles and linear optics. Nature 414: 413-418.

40. Van Loock P (2006) Hybrid quantum repeater using bright coherent light. Phys Rev Lett 96: 240501.

41. Zhao B, Chen ZB, Chen YA, Schmiedmayer J, Pan JW (2007) Robust creation of entanglement between remote memory qubits. Phys Rev Lett 98: 240502.

42. Müller S. Flexible heuristic algorithm for automatic molecule fragmentation: application to the UNIFAC group contribution model. J Cheminform. 2019;11:57. Published 2019 Aug 20. doi:10.1186/s13321-019-0382-3

Supplementary Files

This is a list of supplementary files associated with this preprint. Click to download.

- TablesandFigures.docx